TEST YOUR METAL – REPURPOSING OF THE LIS3MDL MAGNETOMETER FOR FERROUS OBJECT DETECTION ON A ROBOT PLATFORM

Jordan Taylor
1843194

Matthew Crees
1809102

***Abstract*— This paper investigates the sensitivity of the LIS3MDL magnetometer to ferrous material. In conjunction with the Pololu 3Pi+ 32U4 robot, it is demonstrated a mobile platform can converge on a bearing towards a ferrous object.**

I. INTRODUCTION

Mobile robotic platforms are becoming more and more ubiquitous outside of laboratory settings. They have entered our homes and found places in commercial industries [1]. This opens new avenues of opportunity, such as deployment in areas that are inaccessible to humans. This includes environments with extreme temperatures, limited visibility, or very little space. In such situations, alternate forms of spatial awareness may be required alongside traditional visual light sensors. Often these robots are equipped with IMU systems which include small scale magnetometers, so we propose that a magnetometer can fulfil this role. Ferrous objects such as metal furniture and structural supports may be used as navigational anchors [2].

This paper concerns an investigation of the LIS3MDL three-axis magnetometer mounted on the Pololu 3Pi+ 32U4 mobile robot [3]. The 3Pi+ was tasked with locating ferrous objects of varying mass in its local vicinity on the horizontal plane. The accuracy at which the platform correctly identifies objects is explored. This is further extended to compare performance differences between different ferrous alloys, namely pure iron and grade 304 stainless steel.

II. BACKGROUND

The first form of magnetometer was the compass, in which a needle indicates the direction of the local magnetic field. Modern magnetometers are based on the work of Carl Friedrich Gauss and Edwin Hall. The potential difference across a component of the magnetometer varies as a function of magnetic field strength. The resulting potential difference is small so it must be amplified. To measure a magnetic field in real world 3D space, a three-axis magnetometer is required.

A. Pololu 3Pi+ Robotic Platform

This paper concerns the ability of a robotic platform equipped with the LIS3MDL magnetometer to successfully identity ferrous materials (See *Section II.B)*. The Pololu 3Pi+ 32U4 was used as the platform, with the LIS3MDL magnetometer located in the top-left section of the Arduino board, alongside the gyroscope and accelerometer as part of its full IMU unit. The 3pi+ 32U4 control board uses the same microcontroller as the Arduino Leonardo, a well-supported Arduino configuration [4][5].

The Pololu 3Pi+ is roughly circular in shape, with a diameter of 97.0mm, height of 22.4mm, and mass of approximately 100g [3].

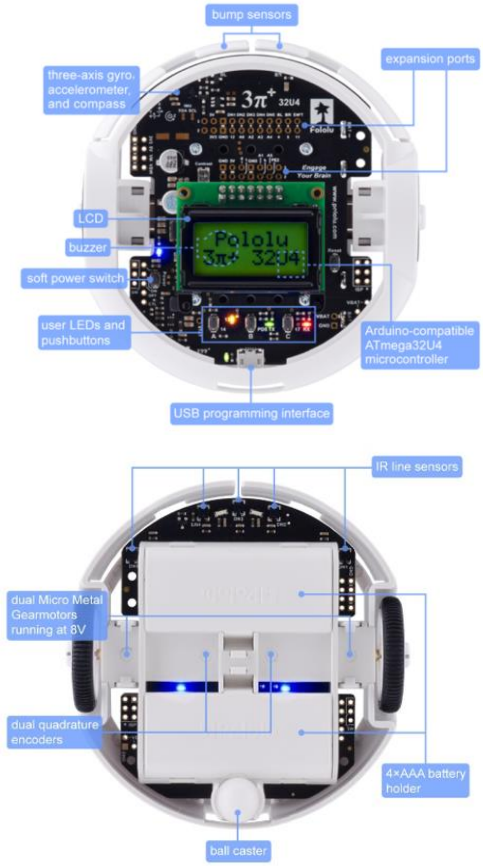

Figure 1: Above and Below labelled view of the Pololu 3pi+ platform.

As seen in *Figure 1*, the platform is equipped with dual micro metal gearmotors running at 8V with a 30:1 gear reduction for the drive system at the central axis – attached to 34mm diameter treaded wheels. This allows for turning on the spot. Each motor is fitted with a dual quadrature encoder for odometry. The robot itself runs at a nominal voltage of 4.8V – 6V, provided by four onboard AAA cells fitted at the underside of the robot [4].

B. LIS3MDL Magnetometer

The magnetometer investigated in this paper is the LIS3MDL: a three-axis hall-effect magnetometer capable of measuring a three-dimensional magnetic field vector. Its small form factor (2.0 x 2.0 x 1.0 mm) permits it to be mounted on an integrated circuit board [4]. This enables the sensor to be included on a variety of small robotic platforms. According to Pololu, the LIS3MDL's usage as a measuring device is not as reliable as larger dedicated magnetometers typical of laboratory settings (LIS3MDL minimum uncertainty ± 4 gauss, with varying sensitivity to the environment). Nevertheless, this paper is primarily designed to determine the

accuracy of the sensor in conjunction with a robot platform, not its precision.

C. Preliminary Magnetometer Readings

Prior to formulating a hypothesis and implementing the series of experiments, the magnetometer was tested to ensure it behaved as expected.

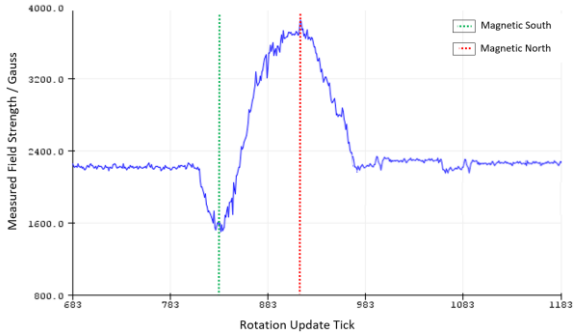

Figure 2: Earth's Magnetic Field Strength Magnitude as Measured in the 3Pi+'s X-Y Plane Over a Full Rotation

The 3Pi+ with equipped LIS3MDL was rotated through 360 degrees on the spot while connected to the Arduino Serial Plotter. The x axis of *Figure 2* represents each datapoint received via the Arduino serial. Rotation update ticks are guaranteed to be separated by at least 30 milliseconds. However, ticks are not representative of real time due to uncertain computational overhead. The magnitude of the Earth's magnetic field vector in the X-Y (flat horizontal) plane as measured by the LIS3MDL is depicted by the y-axis of *figure 2*. Through a full rotation, the magnetic south pole and magnetic north pole can be seen as the graph's minimum and maximum field strength magnitude respectively. As a result, any solution to detect ferrous objects in the horizontal X-Y plane will have to compensate for the ambient magnetic field of the Earth. Furthermore, an important consideration is the fluctuation of field strength magnitude, even when the platform is stationary at rest. The greatest fluctuation was observed to be **300 µ-gauss.** It must be noted that this value is the **magnitude** of the magnetic field vector at the point of the magnetometer, and as such may not be negative.

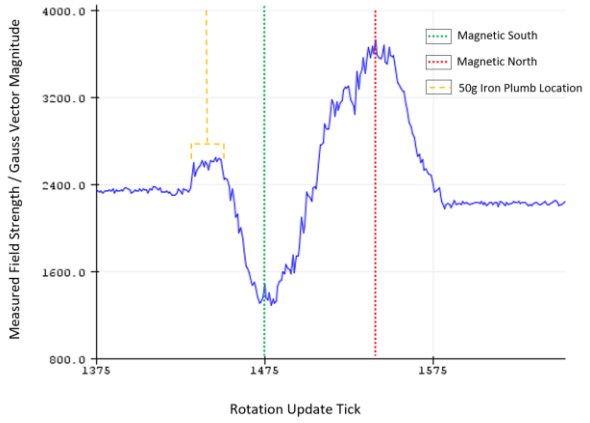

Figure 3: Ambient Recorded Magnetic Field Strength Magnitude with Included Iron Mass

The preliminary experiment depicted in *Figure 2* was repeated, but this time with a 50g solid iron mass placed at 1cm from the 3Pi+ at 10 degrees through its rotation. The results can be seen in *Figure 3.* A noticeable increase in magnetic field strength magnitude can be seen before the large dip as magnetic south is approached. The fact that change is registered by the LIS3MDL demonstrates that it is capable of detecting ferrous objects. This provides a solid basis for further investigation.

D. Hypothesis Statement

As evidenced in the preliminary work in the previous subsection, the LIS3MDL has been identified as a passive sensor capable of detecting a change in the local magnetic field due to ferrous objects, we hypothesise that:

H1: The LIS3MDL magnetometer, with the aid of a mobile robotic platform, will be able to correctly locate ferrous objects in its local vicinity.

H2: The accuracy of the LIS3MDL correctly identifying ferrous objects will increase in proportion with the mass of ferrous object.

H3: Objects with a higher ferrous content will be more reliably detected than those with lower ferrous content.

H4: Objects with higher ferrous content will be more accurately detected than those with lower ferrous content.

To demonstrate the testing of the above hypotheses, the paper is separated as follows: Section III provides details on technical implementation. Section IV describes experimental methodology. Section V presents observations and results. Sections VI and VII discuss the significance of our work, possible future applications in related areas, as well as potential for further work, thus concluding the paper.

III. Implementation

A. Development Environment

The solution was programmed using the Arduino IDE, utilising the Serial Monitor and Serial Plotter for diagnostics and debugging. The LIS3MDL must be calibrated on start-up. During operation, the 3Pi+ rotates on the spot. Ferrous masses are placed at randomly chosen points along the platform's rotation.

B. Odometry and Rotation Tracking

Throughout each experiment, the 3Pi+ must know its current rotation. As such, a closed loop control system must be created to keep track of this value. Each micro metal gearmotor is fitted with a dual quadrature encoder at a 358:1 magnet to shaft rotation ratio [4]. A pair of pin interrupts were defined on the Leonardo board for each encoder, triggered when a voltage is induced by the encoder sensor. By measuring the magnet sensors, each wheel's direction and rotational velocity may be calculated.

C. Magnetic Field Map Construction

One of the challenges faced in creating the ferrous object detector was that of compensating for the magnetic field of the Earth and environment. While searching for ferrous objects, the 3Pi+ takes measurements of the local magnetic field, minus that of an estimated ambient magnetic field at its current rotation, resulting in a filtered field vector. The field vector is used to calculate a relative bearing to the field origin.

The ambient magnetic field estimation is achieved by building a magnetic map of the local area and saving it to memory. When the 3Pi+ is powered on, it proceeds to rotate in 4-degree increments. This continues until a full rotation is completed. After each increment, 100 polls of the magnetometer are taken, and a mean magnetic field vector is calculated. The X and Y components of this vector are saved to volatile memory. The 3Pi+ remains stationary during each sample period to avoid interference with the magnetic fields of the drive motors. Due to the limited RAM of the Leonardo board (~2kB) [5], only 90 pairs of magnetic field components can be stored without encountering memory issues.

Magnetic Map Construction Routine:

1. Calibrate Magnetometer; finds maximum and minimum field strength components.
2. Rotate 4°.
3. Poll magnetometer 100 times, calculate mean magnetic field vector.
4. Save X and Y vector component to memory.
5. Repeat steps 1-4 90 times to give a full 360° rotation.

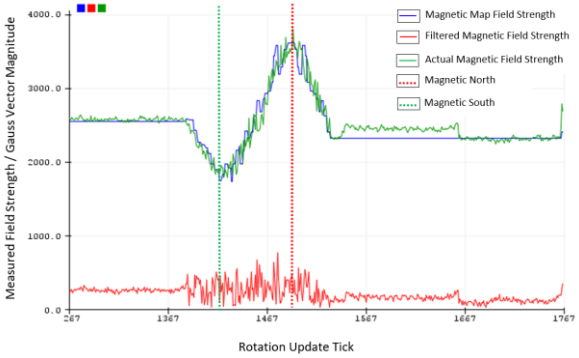

Figure 4: Ambient Recorded Magnetic Field Strength Magnitude Through Full Rotation Filtered by Magnetic Map

The success of the magnetic map can be seen in *Figure 4*. Evident between tick *1367* and *1567*, filtered magnetic field strength appears noisier when the 3Pi+ is rotating compared to when stationary. This is in part due to inaccuracies of the magnetic map being measured discretely. Spikes occur due to the difference in measured values and saved values. Additionally, moving the magnetometer while it is taking samples induces measurement flux and causes a wider range of values to be used in calculating the current magnetic field vector, therefore resulting in more variation of the directly observed field strength.

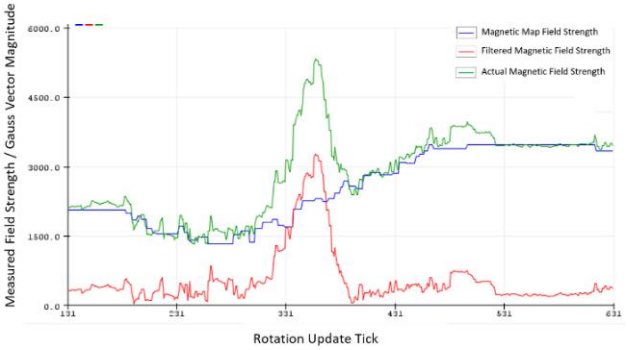

Figure 5: Recorded Magnetic Field Strength Magnitude Through Partial Rotation Filtered by Magnetic Map Over Ferrous Mass

Figure 5 demonstrates successfully identifying a 100g ferrous mass at 1cm from the 3Pi+ while undergoing a partial rotation. The filtered magnetic field strength magnitude exhibits a distinct peak in the presence of the ferrous mass. Background noise returns to baseline after the mass has been passed. As a result, only readings above a threshold magnitude are candidates for identification.

D. Best Orientation Identification and Search Pattern

Filtered magnetic field vectors with magnitude above a background noise threshold are defined as residing within a peak (*figure 5)*. When observed, peak vectors are normalized to be between the maximum and minimum components found during calibration and projected on to the X-Y plane. A bearing from the 3Pi+'s heading relative to the field's origin point is computed. The closer the bearing to North, the more likely the origin of the field, and hence ferrous mass, has been identified. This process is constantly repeated. If a better relative bearing is calculated, the 3Pi+'s current rotation is saved to memory.

The 3Pi+ uses an iterative convergent search algorithm to identify its target, described in *Figure 6*.

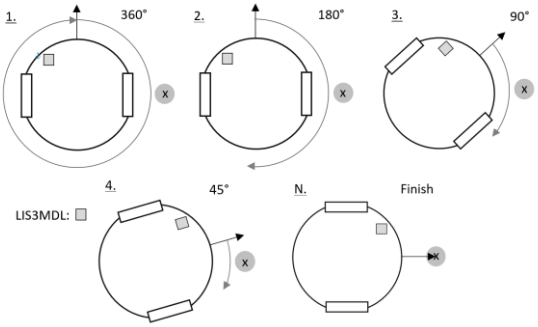

Figure 6: Iterative Convergent Search Pattern Employed by The 3Pi+

The search pattern is designed to improve both identification accuracy and precision. Accuracy is improved by requiring multiple passes over a search arc. False positive best heading identification can be due to noise in the filtered magnetic field reading. The peak area is searched multiple times, thus overriding potentially erroneous readings, and increasing the sample size of heading candidates. The search continues for a predefined number of iterations (defaulting to 15). Each iteration's search arc is halved to give increasing precision. Once completed, the 3Pi+ rotates towards the most likely position of the ferrous object.

IV. Experiment Methodology

This section will explain the experiment procedure used to assess the previously stated hypothesis; covering how to set-up and run the experiment. There are key focuses on the methodology used, the important variables to be considered, and the metrics which will be used to interpret our results.

A. Overview of Method

Figure 7 shows the environment for each run of the experiment. There is a placement marker outlined on the floor that is used as reference to make sure the robot is put in the same position every time, therefore reducing operator error. Specific consideration is given to the Earth's magnetic North. The robot will point towards North when it fails to detect a source of ferrous material. As such, the metal is initially

placed at a heading of 90° away from North so it can be clear when the robot has detected the metal successfully. The distance between the robot and the metal is discussed later in *Section IV.B.*

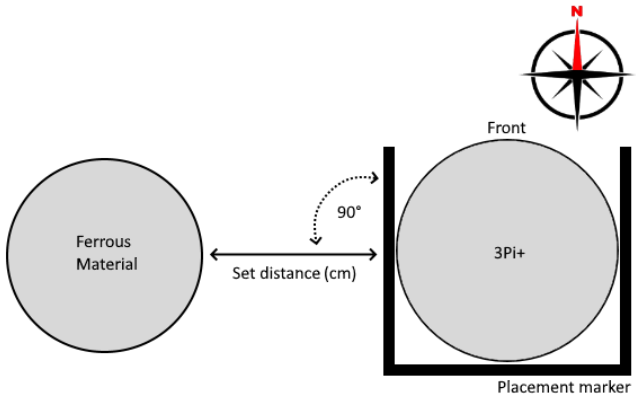

Figure 7: Top-down view of the experiment setup. The robot is placed within a bounding placement marker, facing North. The ferrous material is later placed perpendicular to this at a set distance.

Each run of the experiment follows the steps outlined in Figure 8. These runs have a duration of ~90 seconds:

- Magnetometer calibration: 40s
- Pause for metal placement: 10s
- Searching for ferrous material: 30s
- Operator heading measurement: 10s

8 different masses of metal are tested, from 25g to 200g in 25g increments. 20 runs were performed per mass. This ensured that the results were more reliable and allowed the consistency of the metal detection to be tested accurately. When measuring the heading angle at the end of a run, a protractor and straight edge are used to ensure that the angle is lined up correctly. A measurement is taken from the centre of the robot to the centre of mass of the ferrous material, with the protractor zeroed along a line running through the front of the robot.

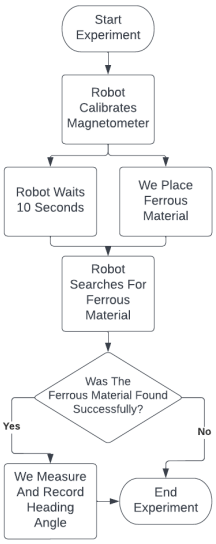

Figure 8: Flowchart of the experiment procedure.

B. *Discussion of Variables*

To have credible and reproducible results, several key variables must be considered. These highlight potential for error. Described below are the measures taken to control variables and mitigate error.

Controlled Variables:

- Robot's starting position, assigned by a placement marker outline with electrical tape. This reduces the chance for operator error when placing the robot.
- The bearing at which the ferrous material is placed from North to ensure successful metal detections are distinct from a false positive.
- The pattern in which rivets/bolts are placed so that the magnetic field does not shift.
- The distance between the robot and ferrous material.
- The same robot is used each time, to eliminate variations between hardware.
- Position of the experimental setup in relation to other objects in the area. Sources of potential magnetic interference should be removed or otherwise moved away from the experiment. Attention should be given to removing electrical devices due to their fluctuating magnetic fields.

Independent Variable(s):

- Primary: Mass of the ferrous material.
- Secondary: Ferrous content in the material.

Dependent Variables:

- Success or failure to detect ferrous material.
- Angle between the centre of mass of the ferrous material and the final heading of the robot upon a successful metal detection.

As the ferrous materials need to be moved away from the robot in the calibration stage of the experiment, there must be a control to ensure the metal does not shift position between runs. The robot searches for the ferrous material's magnetic field origin. Placing the metal in inconsistent arrangements would alter this point. To solve this, a PLA holder was fabricated using a 3D printer (*Figure 9*). It has 8 uniform holes, capable of housing a single steel bolt or 25g of iron rivets. The holder is cylindrical so that the material's magnetic field will remain approximately the same size and shape between trials. Additionally, it is ensured that the centre of mass of the ferrous material will shift less between trials.

Figure 9: CAD of the bolt/rivet holder.

To find the optimal distance to use in the experiments, a preliminary test was carried out. 100g of iron rivets were placed at varying distances from the robot between 2cm and 10 cm, at 1cm increments. At each distance, the robot attempted to find the metal 20 times, and the successful detections were recorded. These results can be seen in *Figure 10*. From this graph, it was decided that 5cm would be the optimal distance to set for the final experiment. This is because it has a hit rate close to 50%, which matched it being in the middle of the range of masses to be used.

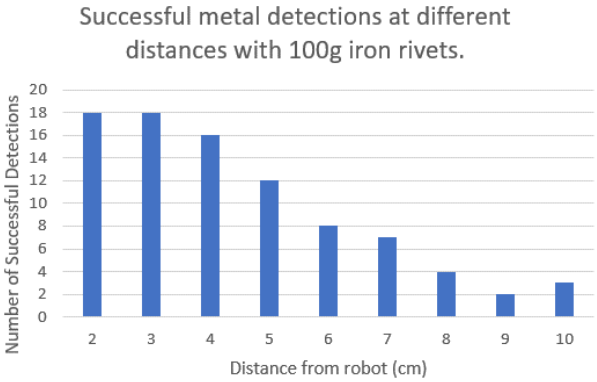

Figure 10: Bar chart showing the relationship between the number of successful metal detections and the distance which the ferrous material is placed from the robot.

In order to make sure that the accuracy tests of the magnetometer better reflect how it may be used in practice, a second set of experiments was conducted using an iron-based alloy. Steel was used due to its ubiquity compared to pure iron in the real world, represented by A2-40 grade 304 stainless steel bolts with ferrous content of 67-71% [6]. The iron rivets are solid ferrous material, giving them a close-to-100% ferrous content, minus any manufacturing impurities.

C. *Discussion of Metrics*

Two metrics are used to help analyse the effectiveness of the LIS3MDL as a metal detector:

1. The hit rate of successful metal detections. This is tracked across the entire range of masses: 25-200g.
2. The range of heading angles where metal detection is successful. This is also tracked across the entire range of masses.

Due to the inherent noise present in the magnetometer readings, it is not expected that the robot will successfully find the target metal during each search trial. As such, the success "hit-rate" will be used to analyse the reliability of using the LIS3MDL to detect ferrous material. The accuracy of the system is further tested by analysing the final heading of the 3Pi+. A smaller range of angles would suggest greater accuracy in identifying the heading towards the ferrous material.

V. Results

A. *Metric 1: Hit Rates of Successful Metal Detection*

Figure 11 shows the results of testing different masses of both the steel bolts and the iron rivets. It shows that the robot is much more reliable at finding the ferrous material as the mass of the metal increases. This supports our hypothesis. It can also be observed that the material does not have to be pure ferrous, as the same behaviour is exhibited when testing the steel bolts and the iron rivets, albeit with fewer successful detections in the alloy.

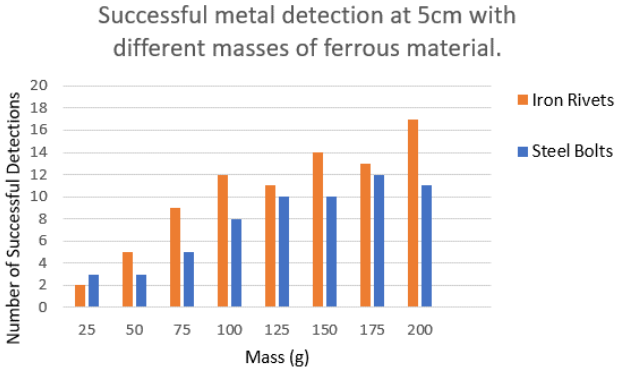

Figure 11: Bar chart showing the relationship between the number of successful metal detections and the mass of the ferrous material. Both iron rivets and steel bolts are shown.

B. *Metric 2: Final Heading Angles*

Figure 12 shows how the angle between the robot's final heading and the center of mass of the ferrous material varied over the course of the experiment. It shows that the robot does not consistently find the center of mass of the ferrous material, but it does not stray further than 10°. Iron rivets have a variance of 9.36, while the steel bolts have a variance of 5.77. The mean final heading found for both metals was -5°, but this offset from 0° is expected behaviour as the magnetometer is not placed centrally on the Leonardo board *(Figure 1)*. As such, its readings will be biased towards one side of the robot's heading.

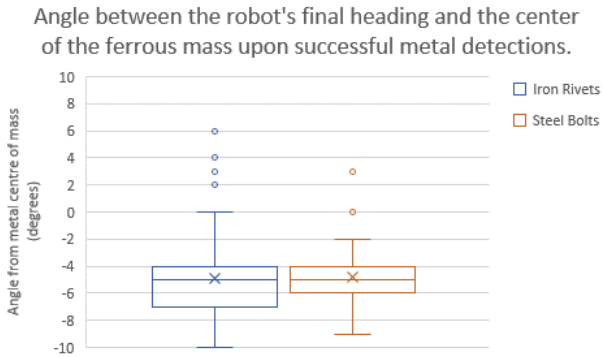

Figure 12: Box-and-whisker plot showing the range of angles between the robot's heading and the center of mass of the ferrous material when metal is successfully detected. Both iron rivets and steel bolts are shown, covering mass over the range 25-200g.

VI. Discussion & Conclusion

The results of the above experiments have supported the hypothesis:

H1: The LIS3MDL magnetometer, with the aid of a mobile robotic platform, will be able to correctly locate ferrous objects in its local vicinity.

H2: The accuracy of the LIS3MDL correctly identifying ferrous objects will increase in proportion with the mass of ferrous object.

H3: Objects with a higher ferrous content will be more reliably detected than those with lower ferrous content.

H4: Objects with higher ferrous content will be more accurately detected than those with lower ferrous content.

Results from the experiment support hypotheses H1, H2 and H3, but H4 appears to be contradicted.

The LIS3MDL, with the aid of the Pololu 3Pi+, successfully locates ferrous objects. Evident in *Figure 11*, detection accuracy rate increases with the mass of ferrous material, from 10% and 15% for 25g of iron and grade 304 steel respectively, to 85% and 55% at 200g. The absolute and relative performance discrepancy between iron and steel broadly grow in favour of iron as object mass increases. This is expected behaviour as per the hypotheses. Exceptions to this are evident in the first trial set. The LIS3MDL appears to identify steel more frequently than iron at 2 to 3 correct identifications of 20. This can be attributed to the small magnetic field size and strength induced by a 25g mass at 5cm away becoming lost in background noise. The system is resilient to false positive results as the 3Pi+ consistently rotates to North on each failed detection attempt. This demonstrates detection accuracy as a function of ferrous material.

Collating all mass experiment data (*Figure 11*); the 3Pi+ has an average hit-rate of 45.3%. This suggests that the 3Pi+ platform is capable of using the LIS3MDL magnetometer as part of a navigational sensor suite to traverse a gap of twice its own width. In similarly sized platforms, this capability may lend itself to search and rescue operations as well as underground navigation in claustrophobic environments. In such situations, larger ferrous objects may represent more pertinent obstacles or targets. The low success rate of detecting small masses may not be overly consequential.

As evidenced in *Figure 12*, there is more variation in the final bearings than what would be preferable. Based on the ferrous content alone, this would appear to be anomalous behaviour. However, it can be explained when considering the shapes of the different metals. The steel bolts are much larger than the iron rivets, with the former being 25g each and the latter being only 2.5g. As such, many more individual rivets were needed for each increment in mass. This meant that there was more chance for the rivets to shift position when placing them down, thus explaining the greater range of heading angles measured. Relying on a magnetometer alone is likely to be too inconsistent for full-scale environment mapping and traversal. A potential aid to this could have been to utilise a PID controller for the drive system. This was not able to be implemented due to insufficient program space in the Leonardo board's memory. As such, there is minor wheel slip and motor power variance when performing the search algorithm causing noise in the calculated bearing. Greater memory availability would permit a more sophisticated movement solution.

Limitations to the study were as follows: there was difficulty in performing the experiments as access to suitable locations was limited. The university facilities have predominantly metal furniture, power cables, and many computers running. These cause significant fluctuating magnetic fields that interfered too much for experiments to be run on campus.

VII. Future Work

Future work could look to explore metal detection while the robot changes location, rather than just rotating on the spot. This may be more complex as any changes in height would require a rework of the magnetic maps. They would need work in 3D, rather than just the 2D horizontal plane. This would require utilising either the gyroscope or the accelerometer. It would also likely need to use a different robotic platform as the memory limitations mentioned previously would again cause issue. Furthermore, work could be undertaken to apply more filters to reduce the noise in magnetometer readings [7]. Magnetic fields due to the drive motors can be accounted for. Different noise reduction methods may be evaluated in regard to increasing detection accuracy, such as implementing fraction filters and moving averages [8].

References

[1] E. Boto, S. S. Meyer, V. Shah, O. Alem, S. Knappe, P. Kruger, T. M. Fromhold, M. Lim, P. M. Glover, P. G. Morris, R. Bowtell, G. R. Barnes, and M. J. Brookes, "A new generation of magnetoencephalography: Room temperature measurements using optically-pumped magnetometers," NeuroImage, vol. 149, pp. 404 – 414, 2017.

[2] Yan, W., Weber, C. and Wermter, S., 2013. Learning indoor robot navigation using visual and sensorimotor map information. Frontiers in Neurorobotics, 7.

[3] Pololu.com. 2022. Pololu 3pi+ 32U4 User's Guide. [online] Available at: <https://www.pololu.com/docs/0J83/all> [Accessed 27 April 2022].

[4] St.com. 2022. [online] Available at: <https://www.st.com/resource/en/datasheet/lis3mdl.pdf> [Accessed 27 April 2022].

[5] Pololu.com. 2022. Pololu - Arduino Leonardo. [online] Available at: <https://www.pololu.com/product/2192> [Accessed 27 April 2022].

[6] Blickman. 2022. Understanding Stainless Steel — Blickman. [online] Available at: <https://www.blickman.com/understanding-stainless-steel> [Accessed 27 April 2022].

[7] Ozyagcilar, T., 2015. Implementing a Tilt-Compensated eCompass using Accelerometer and Magnetometer Sensors. [online] Mikrocontroller.net. Available at: <https://www.mikrocontroller.net/attachment/292888/AN4248.pdf> [Accessed 27 April 2022].

[8] Trimmer, J., Larroumets, A. and Bulsink, E., n.d. Increasing Magnetometer Performance in a Mobile Robot Setup by Noise Reduction Filtering. [ebook] University of Bristol, pp.1-6. Available at: <https://github.com/paulodowd/EMATM0053_21_22/raw/main/Example%20Reports/SG7_T4_IncMagPerf.pdf> [Accessed 27 April 2022